Available online at www.sciencedirect.com

ScienceDirect

IFAC PapersOnline CONFERENCE PAPER ARCHIVE

IFAC PapersOnLine 54-2 (2021) 93–98

A Multi-class Lane-changing Advisory System for Freeway Merging Sections

Salil Sharma* Ioannis Papamichail Ali Nadi***
Hans van Lint* Lóránt Tavasszy* Maaike Snelder*,***

**Department of Transport and Planning, Faculty of Civil Engineering and Geosciences, Delft University of Technology, Stevinweg 1, 2628* CN Delft, The Netherlands *(corresponding author's e-mail: S.Sharma-4@tudelft.nl).*
***Dynamic Systems and Simulation Laboratory, School of Production Engineering and Management, Technical University of Crete, 73100 Chania, Greece*
**** TNO, Anna van Buerenplein 1, 2595 DA The Hague, The Netherlands*

Abstract: Cooperative intelligent transportation systems (C-ITS) support the exchange of information between vehicles and infrastructure (V2I or I2V). This paper presents an in-vehicle C-ITS application to improve traffic efficiency around a merging section. This application balances the distribution of traffic over the available lanes of a freeway, by issuing targeted lane-changing advice to a selection of vehicles. We add to existing research by embedding multiple vehicle classes in the lane-changing advisory framework. We use a multi-class multi-lane macroscopic traffic flow model to design a feedback-feedforward control law that is based on a linear quadratic regulator (LQR). The performance of the proposed system is evaluated using a microscopic traffic simulator. The results indicate that the lane-changing advisory system is able to suppress shockwaves in traffic flow and can significantly alleviate congestion. Besides bringing substantial travel time benefits around merging sections of up to nearly 21%, the system dramatically reduces the variance of travel time losses in the system.

Keywords: lane-changing advisory, LQR control method, merging section, multi-class, traffic congestion, cooperative intelligent transportation system.

1. INTRODUCTION

Traffic congestion on freeways causes large delays and therefore high societal costs. Infrastructural bottlenecks (e.g., merging sections, lane-drops, work zones, etc.) locally cause congestion that may spillback to other parts of the network. When traffic demand exceeds the capacity of a merging section, the latter becomes an active bottleneck which results in the formation of a queue on the near-side lane of a mainline carriageway. The queue then spreads laterally to other lanes and triggers a drop in the discharge flow; a phenomenon known as capacity drop (Cassidy and Bertini, 1999). Data from several studies suggest that traffic flow is unevenly distributed over available lanes of a freeway (Knoop et al., 2010, Wu, 2006). Around a merging section, unbalanced flow distribution might also contribute to traffic breakdown starting on a heavily used lane (i.e. near-side lane) and spreading to other lanes with spare capacity available.

In recent years, technological breakthroughs in communication and automation have enabled us to research and develop new cooperative intelligent transportation system (C-ITS) solutions to help tackle the problem of congestion. This system enables vehicles to exchange relevant information with other vehicles (V2V) or with the road infrastructure (V2I or I2V) using communication technologies in order to create in-vehicle and cooperative systems. Using C-ITS, this paper presents an in-vehicle lane-changing advisory system that aims at improving traffic efficiency by balancing the distribution of flow around merging sections.

Existing research has recognized that the traffic situation in the vicinity of infrastructural bottlenecks can be improved by efficiently assigning traffic flow to available lanes on freeways. Previous studies have developed rule-based approaches (Zhang and Ioannou, 2017, Schakel and van Arem, 2014), optimization-based approaches (Ramezani and Ye, 2019, Zhang et al., 2019), and optimal control theory-based approaches (Markantonakis et al., 2019, Roncoli et al., 2017, Tajdari et al., 2020). However, previous studies solely focus on passenger cars and do not embed multiple vehicle classes in the lane-changing advisory framework. This paper addresses this research gap by incorporating multiple vehicle classes within the optimal control framework that is based on a multi-class multi-lane macroscopic traffic flow model. We use microscopic simulation to evaluate the performance of the proposed controller around merging sections, in contrast to Tajdari et al. (2020), since a microscopic traffic simulator provides a real-world testbed.

To this end, the objective of this study is to propose a multi-class lane-changing controller around a merging section to improve its traffic efficiency. The contributions of this paper are two-fold. We develop a multi-class lane-changing advisory system based on a linear quadratic regulator (LQR); and we evaluate its performance around a merging section using a microscopic traffic simulator.

This paper is structured as follows. We formulate a multi-class lane-changing LQR controller in Section 2. Next, Section 3 describes the approach to implement the proposed

10.1016/j.ifacol.2021.06.014

controller in a microscopic traffic simulation software. Then, Section 4 describes the experimental setup to evaluate the proposed controller. We present and discuss our results in Section 5. We conclude the paper and discuss future works in Section 6.

2. FORMULATING A MULTI-CLASS LANE-CHANGING LQR CONTROLLER

2.1 Traffic System Dynamics Using a Multi-class Multi-lane Traffic Flow Model

Consider a multilane freeway (see Fig. 1) that is subdivided into $i = 0, \dots, N$ segments of length L_i, while each segment is composed of $j = m_i, \dots, M_i$ lanes, where m_i and M_i are the minimum and maximum indices of lanes for segment i. Each element of the resulting grid is denoted as a cell with index (i, j). The model is formulated in discrete time, considering the discrete-time step T, indexed by $k = 0,1, \dots,$ where the time is $t = kT$. It is assumed that $j = 0$ corresponds to the segment(s) including the rightmost lane. In Fig. 1 below, $m_0 = 0$ and $M_0 = 2$. According to the definition, the total number of cells from the origin to segment i is $H_i = \sum_{r=0}^{i}(M_r - m_r + 1)$, and the total number of cells for the whole stretch is $\overline{H} = H_N$.

First of all, we will focus on defining the dynamics of a multi-class traffic system comprising U number of vehicle classes. For every vehicle class u, the conservation of vehicles can be defined as:

$$\frac{\partial \rho_u}{\partial t} + \frac{\partial q_u}{\partial x} = 0, \tag{1}$$

where ρ_u and q_u refer to the class-specific density and class-specific flow at time t and location x, respectively.

Under assumptions of homogeneous and stationary conditions, class-specific density and flow are related as

$$q_u = \rho_u v_u, \tag{2}$$

where v_u refers to the class-specific average speed.

Now, the evolution of density for every vehicle class u in a cell (i, j), proposed in (1), can be cast in discrete form as

$$\rho_u^{i,j}(k+1) = \rho_u^{i,j}(k) + \frac{T}{L_i}\left(q_u^{i-1,j}(k) - q_u^{i,j}(k)\right) + \frac{T}{L_i}\left(f_u^{i,j-1}(k) - f_u^{i,j}(k)\right) + \frac{T}{L_i} d_u^{i,j}(k), \tag{3}$$

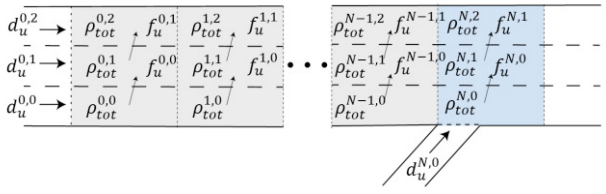

Fig. 1. A hypothetical freeway stretch with an on-ramp

where $\rho_u^{i,j}(k)$ is the density with respect to vehicle class u of a cell (i, j) at time instant k; $q_u^{i,j}(k)$ is the longitudinal flow of vehicle class u leaving cell (i, j) and entering cell $(i+1, j)$ during time interval $[k, k+1)$; $f_u^{i,j}(k)$ is the net lateral flow of vehicle class u leaving cell (i, j) and entering cell $(i, j+1)$ during time interval $[k, k+1)$; and $d_u^{i,j}(k)$ is the external flow of vehicle class u entering the network in cell (i, j) either from the mainline or an on-ramp during time interval $[k, k+1)$.

The discretization should also satisfy the following Courant–Friedrichs–Lewy CFL condition:

$$\frac{L_i}{T} \geq \max\{v_u^{i,j}\}_{u=1,\dots,U}. \tag{4}$$

Since each cell has a mix of vehicle classes, the effective density of a cell (i, j) can be defined using passenger car-equivalents (pce) of vehicle classes:

$$\rho_{tot}^{i,j}(k) = \sum_u \eta_u^{i,j}(k)\rho_u^{i,j}(k), \tag{5}$$

where $\rho_{tot}^{i,j}(k)$ is the effective density of a cell (i, j) at time instant k [pce/km]; and $\eta_u^{i,j}(k)$ is the passenger car equivalent for a vehicle class u in a cell (i, j) at time instant k.

Similarly, total flow in passenger car-equivalents in a cell (i, j) can be defined as:

$$q_{tot}^{i,j}(k) = \sum_u \eta_u^{i,j}(k) q_u^{i,j}(k), \tag{6}$$

where $q_{tot}^{i,j}(k)$ is the total longitudinal flow of vehicle class u leaving cell (i, j) and entering cell $(i+1, j)$ during time interval $[k, k+1)$ [pce/h]; and $\eta_u^{i,j}(k)$ is the passenger car equivalent for a vehicle class u in a cell (i, j) at time instant k.

By combining (3), (5), and (6), the evolution of the effective density of a cell (i, j) can be expressed as

$$\rho_{tot}^{i,j}(k+1) = \sum_u \Big\{\eta_u^{i,j}(k)\rho_u^{i,j}(k) + \frac{T}{L_i}\Big(\eta_u^{i-1,j}(k) q_u^{i-1,j}(k) - \eta_u^{i,j}(k) q_u^{i,j}(k)\Big) + \frac{T}{L_i}\Big(\eta_u^{i,j-1}(k) f_u^{i,j-1}(k) - \eta_u^{i,j}(k) f_u^{i,j}(k)\Big) + \frac{T}{L_i}\eta_u^{i,j}(k) d_u^{i,j}(k)\Big\}. \tag{7}$$

Depending on the network topology, some terms in the above equation may not be present. Lateral flows $f_u^{i,j}$ only exist for $m_i \leq j < M_i$. Thus, the total number of lateral flows terms is $\overline{F} = U(\overline{H} - N)$.

Recall the relationship between macroscopic traffic flow parameters:

$$q_u^{i,j}(k) = \rho_u^{i,j}(k) \cdot v_u^{i,j}(k). \tag{8}$$

Combining (7) and (8), we get

$$\rho_{tot}^{i,j}(k+1) = \sum_u \left\{ \left(1 - \frac{T}{L_i} v_u^{i,j}(k)\right) \eta_u^{i,j}(k) \rho_u^{i,j}(k) + \frac{T}{L_i}\left(\eta_u^{i-1,j}(k) v_u^{i-1,j}(k) \rho_u^{i-1,j}(k)\right) + \frac{T}{L_i}\left(\eta_u^{i,j-1}(k) f_u^{i,j-1}(k) - \eta_u^{i,j}(k) f_u^{i,j}(k)\right) + \frac{T}{L_i} \eta_u^{i,j}(k) d_u^{i,j}(k) \right\}. \quad (9)$$

The proposed control actions are intended for usage prior to the possible onset of congestion, aiming to delay or avoid it. In this case, we may assume that the overall traffic flow entering the controlled area is bounded as it does not exceed the bottleneck capacity and the proposed controller itself can avoid the creation of congestion. Under these assumptions, we consider the following to simplify (9):

1. The average speed in all cells remains at a constant value, i.e. $v_u^{i,j}(k) = v_{crit} \forall i,j,u,k$. Here, v_{crit} refers to the critical speed. All vehicle classes travel with the same critical speed at critical density (Schreiter, 2013).
2. Since speed remains at a constant value, we can also assume fixed passenger car equivalents.
3. Measurable inflows are constant, i.e. $d_u^{i,j}(k) = \underline{d}_u^{i,j} \ \forall \ i,j,u,k$.

Under these assumptions, (9) for two-vehicle classes, cars and trucks, can be reformulated as follows:

$$\rho_{tot}^{i,j}(k+1) = \frac{T}{L_i}(v_{crit}) \rho_{tot}^{i-1,j}(k) + \left(1 - \frac{T}{L_i}(v_{crit})\right) \rho_{tot}^{i,j}(k) + \frac{T}{L_i}\left(\eta_c^{i,j-1} f_c^{i,j-1}(k) - \eta_c^{i,j} f_c^{i,j}(k)\right) + \frac{T}{L_i}\left(\eta_t^{i,j-1} f_t^{i,j-1}(k) - \eta_t^{i,j} f_t^{i,j}(k)\right) + \frac{T}{L_i}\left(\eta_c^{i,j} \underline{d}_c^{i,j} + \eta_t^{i,j} \underline{d}_t^{i,j}\right), \quad (10)$$

where subscripts c and t denote cars and trucks, respectively.

Now the above system in (10) can be considered as a linear time-invariant (LTI) system

$$\underline{x}(k+1) = A\underline{x}(k) + B\underline{u}(k) + \underline{d} \quad (11)$$

where

$$\underline{x} = \left[\rho_{tot}^{0,m_0} \dots \rho_{tot}^{0,M_0} \quad \rho_{tot}^{1,m_1} \dots \rho_{tot}^{N,M_N}\right]^T \in \mathbb{R}^{\overline{H}}, \quad (12)$$

$$\underline{u} = [f_c^{0,m_0} \dots f_c^{0,M_0-1} \quad f_c^{1,m_1} \dots f_c^{N,M_N-1} \quad f_t^{0,m_0} \dots f_t^{0,M_0-1} \quad f_t^{1,m_1} \dots f_t^{N,M_N-1}]^T \in \mathbb{R}^{\overline{F}}, \quad (13)$$

$$\underline{d} = \left[\frac{T}{L_i}\left(\eta_c^{0,m_0} \underline{d}_c^{0,m_0} + \eta_t^{0,m_0} \underline{d}_t^{0,m_0}\right) \dots \frac{T}{L_i}\left(\eta_c^{0,M_0} \underline{d}_c^{0,M_0} + \eta_t^{0,M_0} \underline{d}_t^{0,M_0}\right) \quad \frac{T}{L_i}\left(\eta_c^{1,m_1} \underline{d}_c^{1,m_1} + \eta_t^{1,m_1} \underline{d}_t^{1,m_1}\right) \dots \frac{T}{L_i}\left(\eta_c^{N,M_N} \underline{d}_c^{N,M_N} + \eta_t^{N,M_N} \underline{d}_t^{N,M_N}\right)\right]^T \in \mathbb{R}^{\overline{H}}. \quad (14)$$

This LTI system in (11) can be used to formulate an optimal control problem that is aimed at maximizing traffic efficiency by balancing flows among lanes on a freeway. $A \in \mathbb{R}^{\overline{H} \times \overline{H}}$, composed of a_{rs} elements, represents the connection between pairs of subsequent cells connected by a longitudinal flow and $B \in \mathbb{R}^{\overline{H} \times \overline{F}}$, composed of b_{rs} elements, reflects the connection of adjacent cells connected by lateral flows. These elements are given by:

$$a_{rs} = \begin{cases} 1 - \frac{T}{L_i}(v_{crit}), & \text{if } r = s \text{ and } (i = N \text{ or } m_{i+1} \le j \le M_{i+1}) \\ \frac{T}{L_i}(v_{crit}), & \text{if } r > H_0 \text{ and } s = r - M_{i-1} + m_i - 1 \\ 0, & \text{otherwise} \end{cases} \quad (15)$$

$$b_{rs} = \begin{cases} \eta_c^{i,j} \frac{T}{L_i}, & \text{if } j > m_i \text{ and } (s = r - i) \\ -\eta_c^{i,j} \frac{T}{L_i}, & \text{if } j < M_i \text{ and } (s = r - i + 1) \\ \eta_t^{i,j} \frac{T}{L_i}, & \text{if } j > m_i \text{ and } \left(s = r + \overline{H} - N - i\right) \\ -\eta_t^{i,j} \frac{T}{L_i}, & \text{if } j < M_i \text{ and } \left(s = r + \overline{H} - N - i + 1\right) \\ 0, & \text{otherwise} \end{cases} \quad (16)$$

where $r = H_{i-1} + j - m_i + 1$.

2.2 Optimal Control Problem Formulation

The optimal control minimizes a cost function to steer a system to the desired state. The following quadratic cost function, over an infinite time horizon, has been defined:

$$\min J = \sum_k^{\infty} \left\{ \sum_{\hat{\imath}} \sum_{\hat{\jmath}} \alpha^{\hat{\imath},\hat{\jmath}} \left(\rho_{tot}^{\hat{\imath},\hat{\jmath}}(k) - \hat{\rho}_{crit}^{\hat{\imath},\hat{\jmath}}\right)^2 + \sum_{i=0}^{N-1} \sum_{j=m_i}^{M_i-1} \sum_u \varphi_u^{i,j} f_u^{i,j}(k)^2 \right\}, \quad (17)$$

where $(\hat{\imath},\hat{\jmath})$ are the targeted cells; $\hat{\rho}_{crit}^{\hat{\imath},\hat{\jmath}}$ is the desired set-point; $\alpha^{\hat{\imath},\hat{\jmath}}$ is the weight associated with the targeted cell $(\hat{\imath},\hat{\jmath})$; and $\varphi_u^{i,j}$ is the weight associated with the control actions for a vehicle class u at a cell (i,j). The cost function aims to penalize the difference between selected cell densities and the corresponding pre-defined set points. In addition, it also penalizes excessive lane changes, thus maintaining small control inputs.

Equation (18) can be written in matrix form as follows:

$$\min J = \sum_k^{\infty} \left\{ \left[C\,\underline{x}(k) - \hat{y}\right]^T Q \left[C\,\underline{x}(k) - \hat{y}\right] + \underline{u}(k)^T R\,\underline{u}(k) \right\}, \quad (18)$$

where $Q = Q^T \ge 0$ and $R = \boldsymbol{\varphi} I_{\overline{F}}$ are the weights associated with tracking and control actions, respectively. $\hat{y}$ refers to a vector of set-points and is of dimension $\mathbb{R}^{\overline{Y}}$. C reflects the cells that are tracked. The matrix C is of dimension $\mathbb{R}^{\overline{Y} \times \overline{H}}$. Each row of matrix C contains a single element that

corresponds to the cell that is tracked with the value of one, while the rest of the elements are equal to zero. Since, in this paper, we target only cells in section N, the matrix C can be written as follows:

$$C = [0_{\bar{Y}\times\bar{H}-\bar{Y}}\ I_{\bar{Y}\times\bar{Y}}]. \tag{19}$$

The problem defined in (18) is subject to the linear dynamics presented in (11). Assuming the system is stabilizable and detectable, we can solve this type of problem using a linear quadratic regulator. Since the stabilizability and detectability for such systems have been established in Roncoli et al. (2017), the solution to the proposed optimal control problem can be given by the following linear feedback/feedforward control law:

$$\underline{u}^*(k) = -K\underline{x}(k) + \underline{u}_{ff}, \tag{20}$$

where

$$K = (R + B^TPB)^{-1}B^TPA, \tag{21}$$

$$P = C^TQC + A^TPA - A^TPB(R + B^TPB)^{-1}B^TPA, \tag{22}$$

$$\underline{u}_{ff} = (R + B^TPB)^{-1}B^TF\left(C^TQ\underline{\hat{y}} - P\underline{d}\right), \tag{23}$$

$$F = (I - (A - BK)^T)^{-1}. \tag{24}$$

The feedback gain matrix can be computed offline by solving the Riccati equation. For practical implementation, we may assume that external flows can be measured. In that case, the feed-forward term becomes time-varying. Now, we can rewrite (20) and (23) as follows:

$$\underline{u}^*(k) = -K\underline{x}(k) + \underline{u}_{ff}(k), \tag{25}$$

$$\underline{u}_{ff}(k) = \Phi - \psi\underline{d}(k), \tag{26}$$

where $\Phi = (R + B^TPB)^{-1}B^TF(C^TQ\underline{\hat{y}})$ and

$\psi = (R + B^TPB)^{-1}B^TFP$ may be calculated offline.

3. IMPLEMENTATION OF LANE-CHANGING ADVISORY SYSTEM IN A MICROSCOPIC TRAFFIC SIMULATOR

We assume that there is no latency in V2I or I2V communication at the controller level. The proposed controller requires density measurements for all cells that are considered for the lane-changing advisory system and external demand that arise from outside the system boundaries. To realize the control actions, we keep individual lists of vehicles (cars and trucks) present in those cells. Note that we keep an individual list for every such cell which is of interest to the lane-change controller. Since this is a dynamic list, it gets updated every time a vehicle enters or exits that cell. Depending on the control action, we randomly select the desired number of cars and trucks from the list for a specific cell. These vehicles (cars and trucks) are instructed to follow the lane-change advisory using the lane-changing model (LMRS) (Schakel et al., 2012). Please note that some of the vehicles may not be able to perform lane changes due to the logic of the lane-changing model; however, this limited compliance is balanced by the feedback nature of the proposed controller.

We extend the base LMRS to accommodate a lane change advisory framework in the following equation:

$$d^{y,z} = d_r^{y,z} + \theta_v^{y,z}\left(d_s^{y,z} + d_b^{y,z} + d_a^{y,z}\right), \tag{27}$$

where $d^{y,z}$ is the total/aggregated desire to change lanes. $d_r^{y,z}$, $d_s^{y,z}$, and $d_b^{y,z}$ refer to the desire for following a route, the desire to gain or maintain speed, and the desire to follow a keep-right policy, respectively. Here, $\theta_v^{y,z}$ denotes the weights associated with voluntary motivations. $d_a^{y,z}$ refers to an additional incentive that is triggered if a vehicle receives lane change advice from the control center. This incentive is formulated as follows:

$$d_a^{y,y-1} = \begin{cases} d_{\text{free}}, & \text{if a vehicle receives the lane change advice} \\ 0, & \text{otherwise} \end{cases} \tag{28}$$

$$d_a^{y,y+1} = 0, \tag{29}$$

where y, $y-1$, and $y+1$ refer to the current lane, left lane, and right lane in the direction of driving. Once a vehicle gets lane change advice, it has an additional desire d_{free} to move to its left lane. If the adjacent gap on the left lane is not suitable, the subject vehicle will continue in the current lane. Since we expect vehicles to follow the keep-right policy, we deactivate the subject vehicle's adherence to the keep-right policy ($d_b^{y,z}$) after it passes the merging section.

4. EXPERIMENTAL SETUP

4.1 Study Area

We consider a merging section for the evaluation of the proposed multi-class lane change controller. The merging section (i.e., Ter Heijde) with a 2-lane mainline carriageway is located on the A59 freeway in the Netherlands (see Fig. 2). The acceleration lane is 320 m long. The upstream segment of the considered merging section is 2 km long. We consider three segments, numbered as 0, 1, and 2 in Fig. 2, each 500 m long where vehicles will respond to lane change advisory issued by the control center. The nominal speed limit is 80 km/h for all those segments. This value is also the speed limit for trucks on freeways in the Netherlands.

4.2 Demand Profile

We consider a trapezoidal demand profile for mainline and

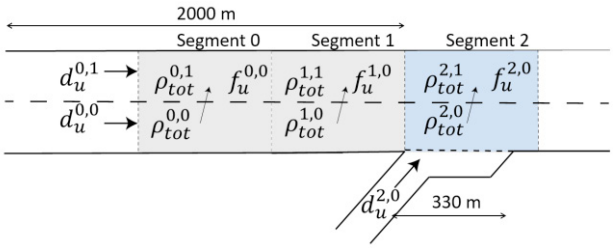

Fig. 2. 2-lane mainline carriageway with an on-ramp

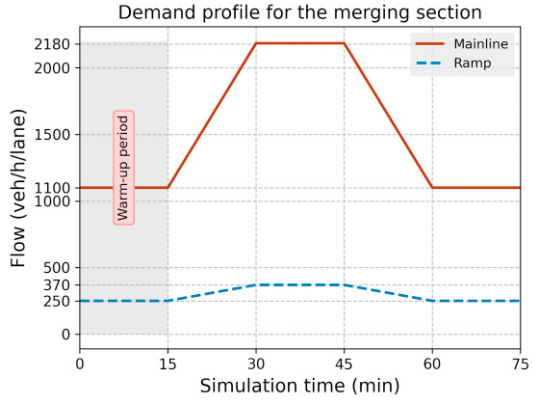

Fig. 3. Demand profile for the experimental setup

ramp traffic (see Fig. 3). The generation time of vehicles in the network follows exponentially distributed headways. The share of trucks is 15% in the traffic mix. All simulations are conducted for 75 minutes of which the first 15 minutes are taken as the warm-up time.

4.3 Simulation Model Parameters

The proposed control strategy is tested using the microscopic traffic simulator OpenTrafficSim. Simulation model parameters are taken from Schakel et al. (2012). For trucks, we use the desired speed distribution (km/h) obtained from a survey, i.e., $v_{\text{des, truck}} = N(84.14, 3.92)$. The lane-changing duration for truck drivers is obtained from a trajectory dataset (van Beinum, 2018) and it follows a normal distribution, i.e. $N(8.32, 2.19)$.

4.4 Scenarios

We consider two scenarios to evaluate the performance of the LQR control-based lane-changing advisory framework.

1. No control: Vehicles do not get lane-changing advisory.
2. LQR control: In this case, mainline vehicles are issued lane change advisory every 20 s. We assume that 100% of vehicles present in the traffic are connected vehicles. For trucks, we use a pce value of 1.61 which is taken from Schreiter (2013) where pce values are calibrated using a trajectory dataset.

4.5 Performance Indicator

We consider the Total Travel Time of the system (TTS in veh·h) as the performance indicator. We do not take warm-up time into account to compute the TTS. TTS can be mathematically expressed as:

$$\text{TTS} = \sum_{i=1}^{N} (t_{exit}^{i} - t_{enter}^{i}), \tag{30}$$

where t_{enter}^{i} and t_{exit}^{i} refer to the time instant a vehicle i enters and exits the network, respectively. N denotes the total number of vehicles that have passed through the merging section in the simulation period.

5. RESULTS AND DISCUSSION

In the scope of this work, we target only cells in segment 2 of the merging section. For both the near-side and off-side lanes at segment 2, we use 41 pce/km/lane as set-points that is closer to their critical density values. The weights of the LQR controller are obtained using a trial-and-error approach ($Q = 10^3 I_2$ and $R = 10^1 I_6$).

The performance of the LQR controller, in terms of TTS, is evaluated over 10 simulation runs (see Fig. 4). We obtain a TTS value of 73.04 veh·h for the no-control case. In comparison to the no-control case, we obtain an average TTS equal to 57.74 veh·h in the controlled case which is a 21% improvement (t-statistic = 4.63, p-value = 0.00). The variance is significantly reduced in the control scenario thus indicating the consistent performance of the proposed advisory system.

In Fig. 5, we present a qualitative evaluation of the performance of the LQR controller for an average scenario. We can observe that the LQR controller is able to suppress shockwaves in the system. Furthermore, density values for both near-side and off-side lanes seem to lie around set-points chosen for the LQR-control case compared to the no-control case. In the LQR control case, the distribution of traffic is more balanced since we observe similar density profiles for both lanes at segment 2. Interestingly, we observe a dip in density between 35-45 minutes. Fig. 6 shows a similar dip in traffic demand between 35-45 minutes. The results suggest that the buildup of density on the near-side and off-side lane follows the traffic pattern under the LQR control scenario. The LQR controller recognizes the randomly distributed demand (or generation of vehicles in the network) and effectively balances the distribution of traffic on both lanes.

6. CONCLUSIONS AND FUTURE WORKS

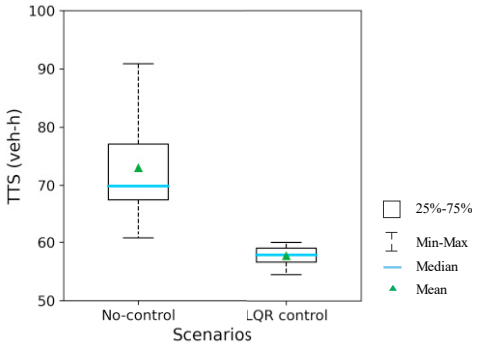

Fig. 4. Comparison of no-control and LQR control scenario

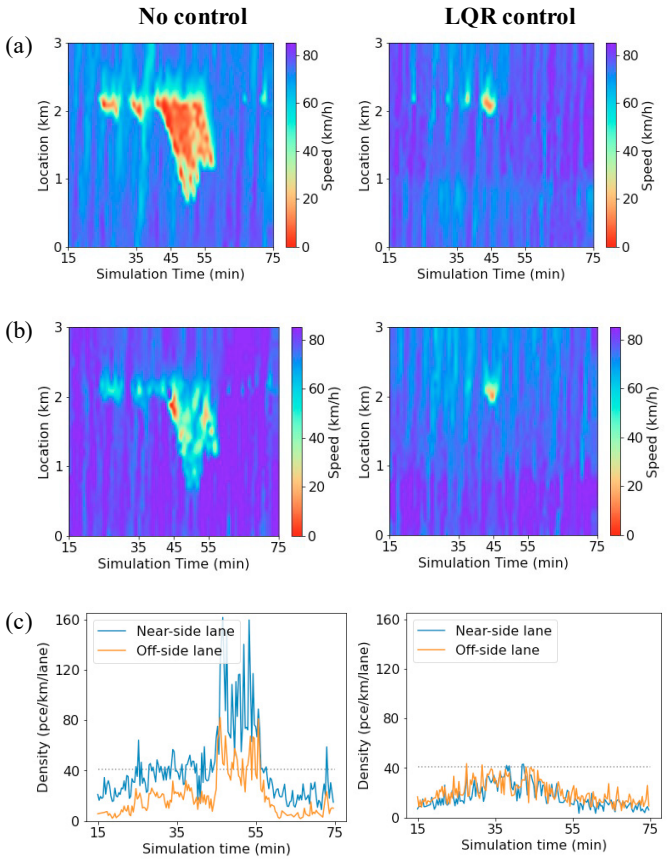

Fig. 5. Qualitative assessment of the LQR controller's performance for an average scenario (a) speed contour plots for the near-side lane (b) speed contour plots for the off-side lane, and (c) lane-specific density profiles at segment 2

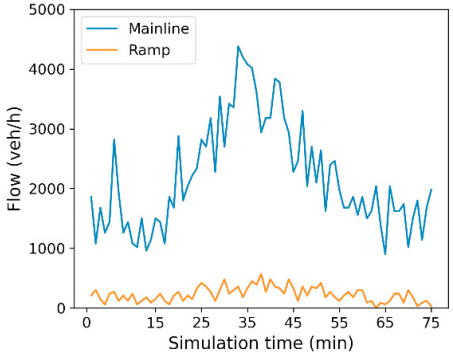

Fig. 6. Demand profile generated for an average scenario under the LQR control case

This paper develops and evaluates a multi-class lane-changing advisory system based on a linear quadratic regulator. The results of microscopic simulations indicate that this system can improve traffic efficiency around a merging section. The findings will be of interest to traffic management agencies and logistics companies which are especially concerned about the travel time reliability of freight corridors. A promising research direction can be to include automated vehicles in the traffic mix. Further, the effectiveness of the proposed system can be evaluated for a scenario that includes truck platoons along with passenger cars and trucks.

ACKNOWLEDGEMENTS

This work was supported by the Dutch Research Council (NWO), TKI Dinalog, Commit2data, Port of Rotterdam, SmartPort, Portbase, TLN, Deltalinqs, Rijkswaterstaat, and TNO under the project "ToGRIP-Grip on Freight Trips".

REFERENCES

Cassidy, M. J. and Bertini, R. L. (1999). Some traffic features at freeway bottlenecks. *Transportation Research Part B: Methodological,* 33(1), 25-42.

Knoop, V. L., Duret, A., Buisson, C., and van Arem, B. (2010) Lane distribution of traffic near merging zones influence of variable speed limits. In *2010 13th IEEE International Conference on Intelligent Transportation Systems (ITSC)*, 485-490. IEEE.

Markantonakis, V., Skoufoulas, D. I., Papamichail, I., and Papageorgiou, M. (2019). Integrated traffic control for freeways using variable speed limits and lane change control actions. *Transportation Research Record,* 2673(9), 602–613.

Ramezani, M. and Ye, E. (2019). Lane density optimisation of automated vehicles for highway congestion control. *Transportmetrica B: Transport Dynamics,* 7(1), 1096-1116.

Roncoli, C., Bekiaris-Liberis, N., and Papageorgiou, M. (2017). Lane-changing feedback control for efficient lane assignment at freeway bottlenecks. *Transportation Research Record,* 2625.

Schakel, W. J., Knoop, V. L., and van Arem, B. (2012). Integrated lane change model with relaxation and synchronization. *Transportation Research Record,* 2316(1), 47-57.

Schakel, W. J. and van Arem, B. (2014). Improving traffic flow efficiency by in-car advice on lane, speed, and headway. *IEEE Transactions on Intelligent Transportation Systems,* 15(4), 1597-1606.

Schreiter, T. (2013). *Vehicle-class specific control of freeway traffic.* Doctoral dissertation, TU Delft.

Tajdari, F., Roncoli, C., and Papageorgiou, M. (2020). Feedback-based ramp metering and lane-changing control with connected and automated vehicles. *IEEE Transactions on Intelligent Transportation Systems*, doi: 10.1109/TITS.2020.3018873.

van Beinum, A. (2018). Freeway turbulence - empirical trajectory data. 4TU centre for research data.

Wu, N. (2006). Equilibrium of lane flow distribution on freeways. *Transportation Research Record,* 1965, 48-59.

Zhang, C., Sabar, N. R., Chung, E., Bhaskar, A., and Guo, X. (2019). Optimisation of lane-changing advisory at the freeway lane drop bottleneck. *Transportation Research Part C: Emerging Technologies,* 106, 303-316.

Zhang, Y. and Ioannou, P. A. (2017). Combined variable speed limit and lane change control for highway traffic. *IEEE Transactions on Intelligent Transportation Systems,* 18(7), 1812-1823.